Effect of Expandable Graphite Particle Size on the Flame Retardant, Mechanical, and Thermal Properties of Water-Blown Semi-rigid Polyurethane Foam

Yi Li,[1] Jing Zou,[1] Shengtai Zhou,[1] Yang Chen,[1] Huawei Zou,[1] Mei Liang,[1] Wenzhou Luo[2]

[1]The State Key Laboratory of Polymer Materials Engineering, Polymer Research Institute of Sichuan University, Chengdu 610065, People's Republic of China
[2]The General Design Department of SCAAT, Chengdu 610199, People's Republic of China
Correspondence to: H. Zou (E-mail: hwzou@163.com); M. Liang (E-mail: liangmeiww@163.com)

ABSTRACT: Different particle size of expandable graphite (EG) were incorporated into water-blown semi-rigid polyurethane foams (SPFs), which acted as the fire shield, in order to enhance the fire retardant properties. In this study, the particle size of EG was systematically varied from 70 μm to 960 μm. The effect of EG particle size on the density, mechanical properties, and thermal stability of SPFs was also investigated. Results showed that EG with smaller particle size showed almost no effect on the fire retardant properties of SPFs while the larger particle size of EG could effectively enhance it. It was observed that the flame retardancy of the composite improved with the increase of EG size which was attribute to the formation and densification of isolation layer with the increase in volume of expanded graphite. Limiting oxygen index (LOI) value of EG/SPF composites increased linearly by two steps with the increase in EG particle size. Horizontal burning test confirmed the above conclusion. Thermogravimetric analysis (TGA) indicated that EG particles and its size exhibited minor effect on the thermal stability of the SPF composites. Moreover, SPF filled with medium particle size of EG (about 400 μm) exhibited a poor compression performance compared with the others. © 2013 Wiley Periodicals, Inc. J. Appl. Polym. Sci. **2013**, *000*, 39885.

INTRODUCTION

Semi-rigid polyurethane foam (SPF) is widely investigated as an important part of the polyurethane foam, which can be used as interior materials of automobile, industrial cushioning material and packaging materials.[1] It is the same as other types of polyurethane foams that changing the types of raw materials and compositions will significantly alter the structure and the subsequent performance of the products.[2] In addition, both open-cell and close-cell structures are existed in SPFs which endow the SPF better sound and vibration attenuation properties.[3] However, the open-cell structure and low degree of crosslinking and chemical structure of SPF will significantly impair its fire retardant ability.[4] SPFs are flammable and will emit high degrees of toxic fumes when subject to combustion, which is perilous to human health. The application of SPF is greatly limited unless the flame retardant properties are evaluated.

Graphite intercalation compound (GIC), has been developed rapidly in recent years. Expandable graphite (EG) is prepared by the intercalation of a variety of intercalation agents[5,6] and can be rapidly exfoliated, to some extent, hundreds of times over its initial volume when subjected to high temperature, forming a worm-like morphology. Therefore, EG is widely used as the flame retardant additives in polyurethane foams (PUF)[7–16] and polymer based composites[17–19]] due to its intumescent nature as a halogen-free flame retardant.[20] Unfortunately, most of these studies are focused on the rigid polyurethane foam, whereas EG modified semi-rigid or flexible polyurethane foams are fewer reported. As an intumescent flame-retardant, the particle size of EG greatly affects the flame retardant properties of polyurethane foams. Shi et al.[21] used an ultra-high-speed mixer to study different-sized EG modified high-density rigid polyurethane foams (RPUF). In their study, they used pulverization time instead of actual size to distinguish EG. It was concluded that RPUF filled with EG as received and that pulverized for 4 min showed a great improvement of fire-retardant performance while EG pulverized for 13 min showed negligible improvement compared with pure RPUF.

The purpose of this investigation is to study the effect of EG with a wide range particle size from 70 μm to 960 μm on the low density water-blown SPFs, such as flame retardancy, thermal stability and compression properties. Density and morphology of EG/SPF composite were also reported and discussed based on the particle size of EG in this article.

EXPERIMENTAL

Raw Materials

(1) Polyol 3050A, a trifunctional polyether polyol, was purchased from GaoQiao Petro. Co. (Shanghai, China). The primary material properties of 3050A are as follows, hydroxyl number, 55.8 mg KOH/g, maximum water content, 0.05 wt %, pH value, 6.5. (2) Polymethylene polyphenyl isocyanate (PAPI) was supplied by BASF. The NCO wt % and average functionality is 30.5 and 2.7, respectively. (3) Chain extender, low molecular weight alcohol with a functionality of 2 and average molecular weight of about 62 g/mol was synthesized in our laboratory. (4) Dabco DC 5188 used as a surfactant was provided by Air product (China). (5) Dabco 2040 catalyst and stannous octoate which were employed for the formation of urethane and cyclotrimerization of isocyanate were provided by Air product (China) and Kelong Chemical Co. (Chengdu, China). (6) Distilled water was used as blowing agent in this study. The reaction formula is as follows:

$$-RNCO + H_2O \longrightarrow -R-\overset{\overset{\displaystyle H}{|}}{N}-\overset{\overset{\displaystyle O}{\|}}{C}-OH \longrightarrow -NH_2 + CO_2\uparrow$$
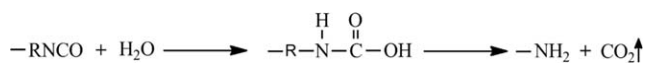
(7) Expandable graphite (sulfur-free), with a broad particle size distribution, was provided directly by the manufacturer. Main properties are presented in Table I.

All materials are used as received.

Foam Preparation

EG was sieved into nine different kinds of particle size by a series of grading sieve before the foam preparation process. The average particle sizes of EG used in this study were 70, 180, 210, 275, 337, 430, 540, 690, and 960 μm, respectively. For simplicity, SPFs containing EG with different particles are designated as S_{70}, S_{180}, S_{210}, S_{275}, S_{337}, S_{430}, S_{540}, S_{690}, and S_{960}, respectively.

The EG-filled SPFs were prepared by a one-shot, free-rise method. The chemical compositions used to prepare the EG/SPF composite in this study are presented in Table II. The

Table I. Main Properties of Expandable Graphite Used in this Study

Properties	Parameter
Density (g/cm^3)	2.2
Ash (%)	0.9
Moisture (%)	0.6
Volatile (%)	10
pH value	7.0
Expansion rate (mL/g)	230
Initial expansion temperature (°C)	About 160

Table II. Chemical Compositions of Water-Blown EG/SPF Composite

Component	pphp[a]
Polyol 3050A	100
Chain extender	6
Dabco DC 5188	2
Dabco 2040	2
Stannous octoate	0.3
Distilled water	2.5
PAPI	81
EG (Different particle size)	20

[a] pphp, parts per hundred parts of polyol by weight.

obtained water-blown SPF was differentiated by the particle size of the loading EG. In addition to PAPI and EG, all the raw materials were mixed in a plastic beaker, then EG was added and the mixture was stirred for 3 min with the help of an electric stirrer. Subsequently, the PAPI was added and the whole mixture was uniformly stirred for 20 s at room temperature, and then the mixture was quickly poured into a cube mold with a dimension of 250 mm × 250 mm × 250 mm. Finally, the foams were aged at room temperature for 24 h before characterizations. In this study, all the EG/SPF samples were prepared with EG loading content of 20 pphp. Samples were cut into required shape for evaluation of different properties.

Characterization

Density. The apparent density tests were carried out according to standard ISO 845:2006. The values of the apparent density were calculated as mass/volume ratio.

Scanning Electron Microscopy and Ultra-Depth Microscope. The morphology of the foams was examined through a scanning electron microscope (SEM, JSM-9600, JEOL, Japan) and an ultra-depth microscope (VHX-1000, KEYENCE, Japan). All materials were cut into small flakes with a blade and then sputter-coated with gold for SEM observations. The accelerating voltage was 5 kV.

Limiting Oxygen Index and Horizontal Burning Test. The limiting oxygen index (LOI) was measured by a HC-2 oxygen index test instrument (Jiangning, China) according to standard ISO 4589-2:1996 with a sheet size of 125 mm × 10 mm × 10 mm. The horizontal burning test was conducted according to UL-94 with a sheet size of 125 mm × 13 mm × 10 mm.

Thermo Gravimetric Analysis. Thermogravimetric measurements were conducted with a thermogravimetric analyzer (TG 209F1 Iris, NETZSCH, Germany) to investigate the thermal stability of the samples under dry nitrogen gas with a flow rate of 60 mL/min. Approximately 4 mg samples were heated at a rate of 10°C/min and the relative mass loss of the samples was recorded from 50°C to 700°C.

Mechanical Test. The compression strength and modulus of all samples were measured with a universal electronic tensile machine (Instron 5507). The size of the specimen was 30 mm
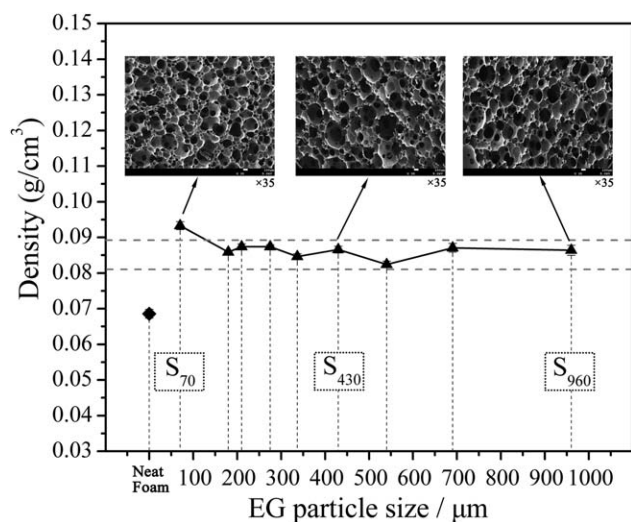
Figure 1. Effect of different particle size of EG on the density of SPF composites.

ascribed to the higher density of EG (2.2 g/cm^3) than that of neat SPF. Density is a key element of polyurethane foam materials, which is directly determined to its performance and applications. It has been demonstrated that strength, modulus and energy absorption abilities of a material improve linearly with the increase of foam density.[22]

The loading of EG with various particle size showed slight impact on the density of SPFs. The S_{70} composites exhibited the highest density compare to other systems, which was due to the fact that the smaller particle size of EG has a "nucleating" effect during the foam formation. As showed in Figure 1, the average cell size of S_{70} is smaller than that of S_{430} and S_{960}.

Morphology

Figure 2(a) shows the SEM cell micrograph of pure SPF. The cell shape is approximately spherical, and open-cell structure can be found in the SPF. Besides, no collapse was observed in the cell system, indicating that the unfilled foam had a uniform and complete cell structure. As shown in Figure 2(b,c), the small graphite flakes was wrapped in the SPF matrix. Figure 2(d,e) demonstrated that larger graphite did not locate in the struts but between the cell walls when the mean particle size of EG was in the same order as the mean size of the cell. This result is in good agreement with the study of EG-containing rigid polyurethane foam,[10] who observed that EG particles laid between cell walls when the mean size of EG particles is of the same order as the mean cell size of the foam. Figure 2(f) showed the interfaces existed between the graphite flakes and SPF matrix, indicating the poor interactions of them.

× 30 mm × 30 mm and the rate of compression process was set at 3 mm/min for each sample. The compressive stress at 25% strain in parallel to the foam-rise direction was performed according to standard ISO 844:2004.

RESULTS AND DISCUSSION

Density

Figure 1 shows the effect of different particle size of EG on the density of SPF. It indicated that the addition of EG caused an increase of density compared to neat foam, which was mainly

Figure 3 presents the ultra-depth optical micrographs of the cross-sections of the S_{70}, S_{430}, and S_{960}, respectively. Results
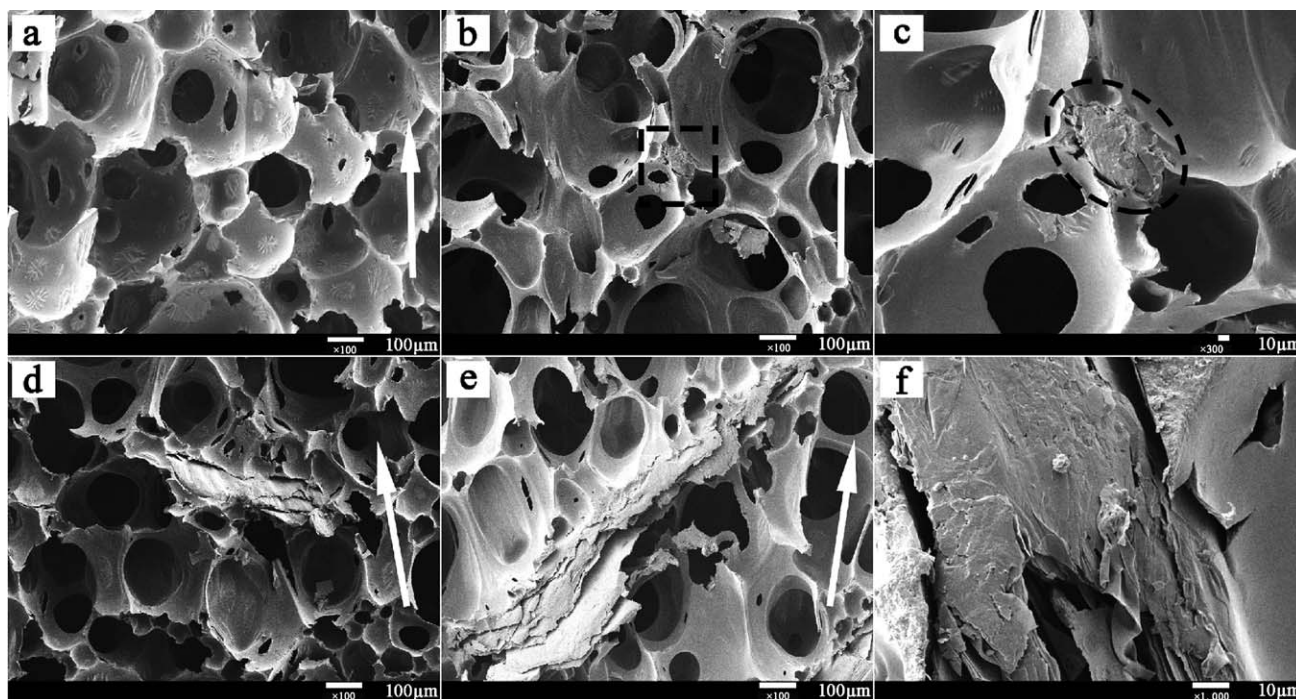

Figure 2. SEM micrographs of pure SPF and EG/SPF composites. (a) Pure SPF (100×); (b) S_{70} (100×); (c) Magnified image of part of (b) (300×); (d) S_{430} (100×); (e) S_{960} (100×); (f) The interface between graphite flakes and SPF matrix (1000×).
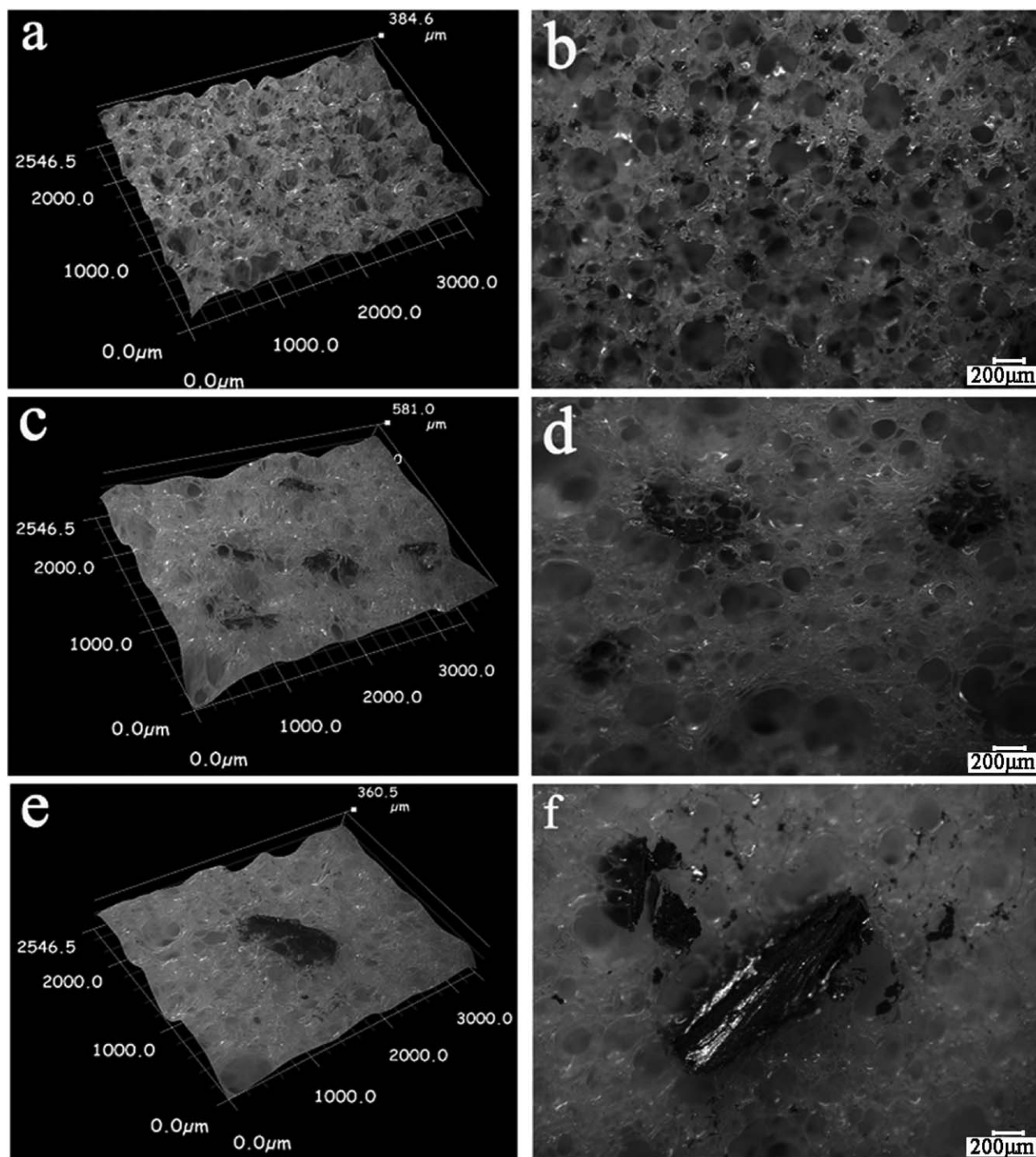
Figure 3. Ultra-depth micrographs of SPF with different particle size. (a, b) S_{70}. (c, d) S_{430}. (e, f) S_{960}.

showed that the increase in particle size of EG led to a decrease of graphite particle numbers at the same addition. It is also seen that smaller graphite flakes dispersed uniformly in SPF while the larger graphite crossed multiple cells and distributed sparsely between the cells. Furthermore, it could be deduced from Figure 3(f) that the stirring process during the foam preparation had a damaging effect on the larger graphite flakes.

Flame Retardant Properties

Limiting oxygen index (LOI) and horizontal burning tests were employed to investigate the fire-retardant properties of EG/SPF composites.

Limiting Oxygen Index. The LOI of pure SPF and EG/SPF composites is shown in Figure 4. The results confirmed our expectancy that larger particle size of EG was beneficial to the flame retardant properties of SPFs. It is illustrated in Figure 4
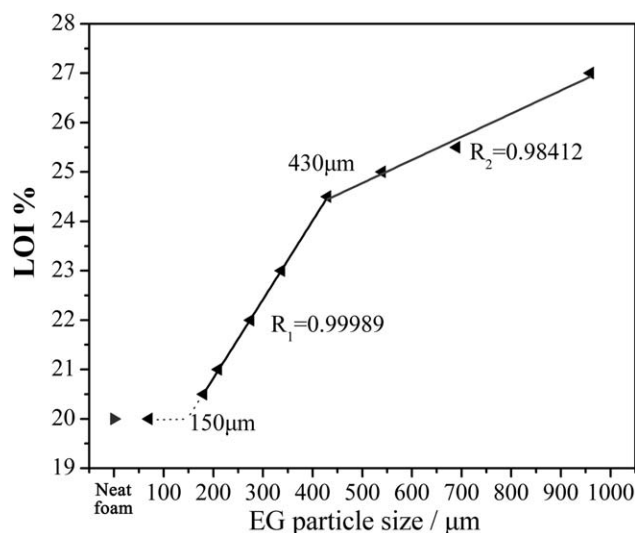
Figure 4. LOI results of SPF with different particle size of EG (20 pphp).

that the LOI value of S_{70} is 20%, which was the same as the neat foam, indicating few effects on fire retardant properties for SPF. The turning point of the LOI curve at graphite particle size of about 150 μm can be deduced from the figure. Moreover, it is obvious that the LOI value of EG/SPF composites increases linearly by two steps after the particle size of EG greater than about 150 μm. The two steps can be equated as follows:

$$\text{LOI} = 17.63 + 0.01595 \, D_{EG} \quad 150 \, \mu\text{m} \leq D_{EG} \leq 430 \, \mu\text{m}. \quad (1)$$

$$\text{LOI} = 22.43 + 0.00469 \, D_{EG} \quad D_{EG} \geq 430 \, \mu\text{m} \quad (2)$$

Where D_{EG} = the particle size of EG (μm).

It is conjectured in this study that while the EG particle size is small, expanded graphite which formed after fire treatment could not form a sufficient barrier layer to hinder the heat penetration process for improving the flame retardancy of EG contained composites (see "Flame Retardant Mechanism" section). However, when the particle size of EG reached about 150 μm, the effective barrier layer formed by the expansion of EG came into effect. When the particle size is bigger than 150 μm, the expanded volume became larger and the flame retardant properties of the sample increased with the increase of EG particle size. But the LOI value of the samples increased slowly when the EG particle size was larger than 430 μm. The slope value of the curve decreased from 0.01595 to 0.00469. This might be explained that the decrease of EG particle number was not beneficial to the formation of compact isolation layer during the fire treatment process.

Horizontal Burning Tests. The results of the horizontal burning tests are tabulated in Table III. The small particle size of EG showed few effect on fire retardant properties of SPF. The horizontal burning rate of the sample gradually decreased with the increasing of graphite particle size. When EG particle size reached to 430 μm, the horizontal burning rate dropped to 15.5 mm/min, reaching the horizontal burning test of HB-3 rating. While further increasing the particle size of EG, the sample reached the HB-1 rating. Figure 5 showed the images of the horizontal burning test, indicating that the larger volume expansion of EG after fire treatment could effectively prevent the fire spreading.

The horizontal burning test is in good agreement with the LOI testing. The data also proved that EG with larger particle size could efficiently improve the fire retardant properties of SPF. The particle size at 430 μm is also an important turning point, which is correspondent to the LOI test results.

Flame Retardant Mechanism

The flame-retardant mechanism of EG in SPF is believed to be the same as in other polymer systems. As clearly depicted in Figure 6, the self-extinguished EG/SPF composites can be divided into three layers: burned layer (matrix was almost completely degraded, EG was complete expansion and exposed), the surface layer (formed by partially expanded EG and partially degraded matrix) and inside layer (internal undamaged layer). When the sample is subjected to fire, the external graphite was rapidly expanded to a worm-like morphology, and the volume increased more than 200 times instantly. The worm-like expanded graphite, which is shown in Figure 7, was embedded in the surface and formed a barrier layer on the heating surface. This burned layer could hinder the oxygen diffusion and limit the heat penetration, which prevented the matrix from further degrading. Similar results were reported by Modesti et al.[8]

In Figure 7, EG with large particle size exhibited larger volume expansion after fire treatment, which is beneficial to the formation of the isolation layer, facilitating the fire retardant properties of SPFs. It can be found in Figure 8, when the particle size of EG reached to 430 μm, the after-combustion volume of the composite became apparent, which was favorable to the fire retardancy of SPF.

Thermal Stability

Figure 9 shows the thermogravimetric (TG) and derivative curves (DTG) behavior of pure SPF and SPFs with three different particle size of EG under nitrogen. Both the neat and EG-containing samples took two-step degradation process from nearly 230–400°C. According to previous studies,[23,24] the first

Table III. Results of Horizontal Burning Tests for SPF with Different Particle Size of EG

Sample	Neat	S_{70}	S_{180}	S_{210}	S_{275}	S_{337}	S_{430}	S_{540}	S_{690}	S_{960}
HB rate mm/min	72.9	70.3	59.8	53.6	48.1	42.3	15.5	–	–	–
Rating	–	–	–	–	–	–	HB-3[a]	HB-1[b]	HB-1	HB-1

[a] HB-3, the burning rate is less than 40 mm/min.
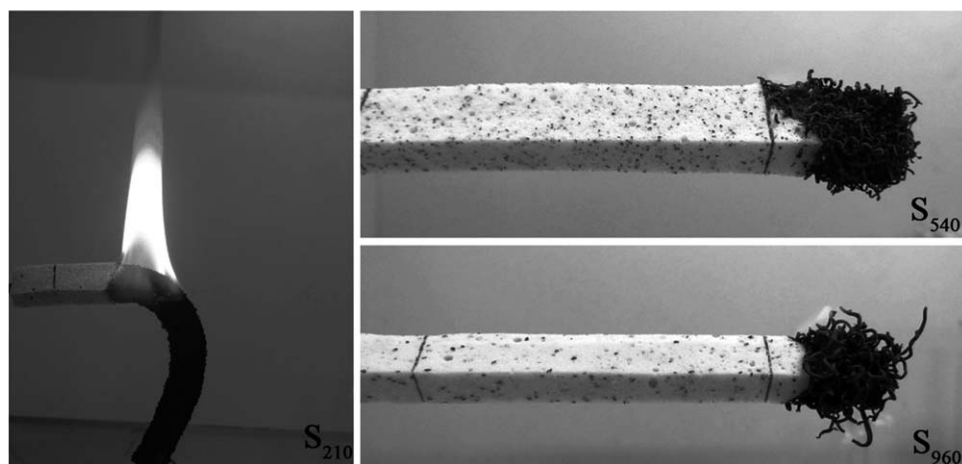[b] HB-1, the flame front does not pass the 25 mm reference mark and quenches after the ignition source is removed.

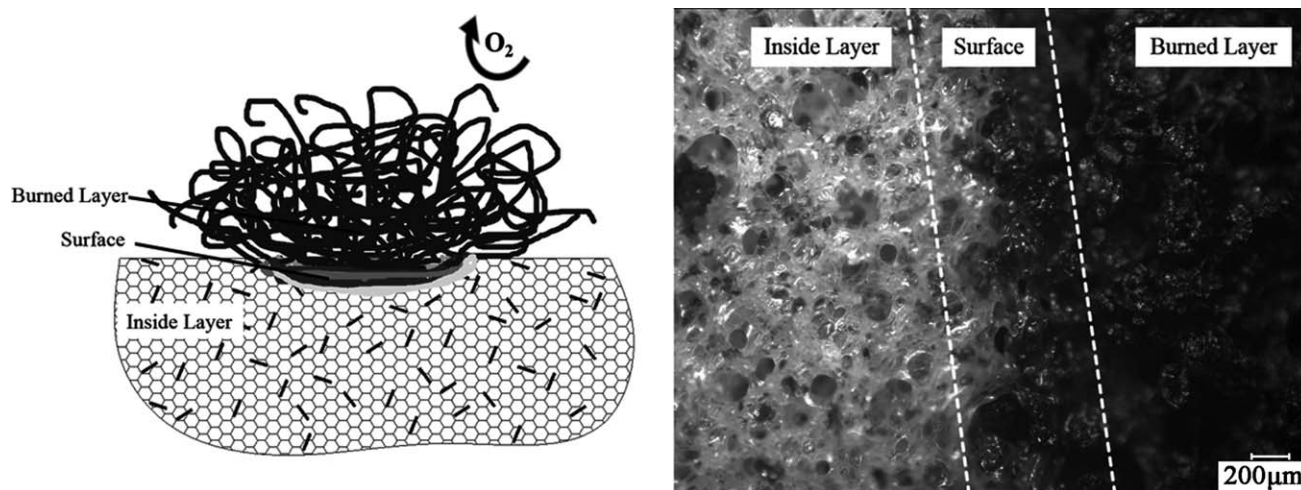**Figure 5.** Images of horizontal burning testing of EG/SPF composites.

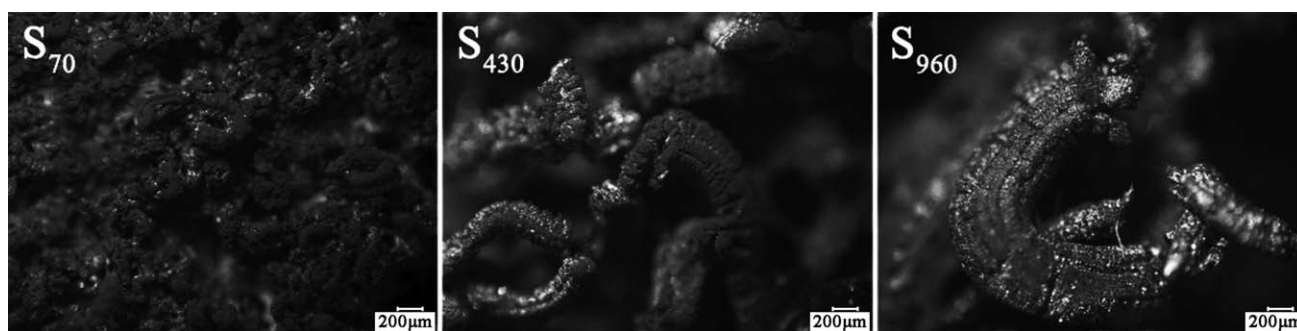**Figure 6.** The EG/SPF composites after self-extinguishing.

Figure 7. Ultra-depth micrographs of the burned layer (expanded graphite).

stage of degradation between 200 and 260°C occurs at urethane hard segment, resulting in the formation of isocyanate and alcohol, primary or secondary amine and olefin, and carbon dioxide. The second stage between 320 and 440°C was corresponding to the thermal decomposition of the soft segment. The higher rate of the second stage was attribute to the high content of soft segments in the SPF.[23] Table IV listed the representative thermal analysis data of the samples. The initial decomposition temperature ($T_{5wt\%}$) is the temperature at 5% weight loss, while the maximum weight loss temperature (T_{max}) is taken from the peak value of the DTG thermograms. Results revealed that EG with small particle size had a positive effect on $T_{5wt\%}$ of SPF systems, while larger particle size of EG was detrimental to the thermal stability of the composite. This can be
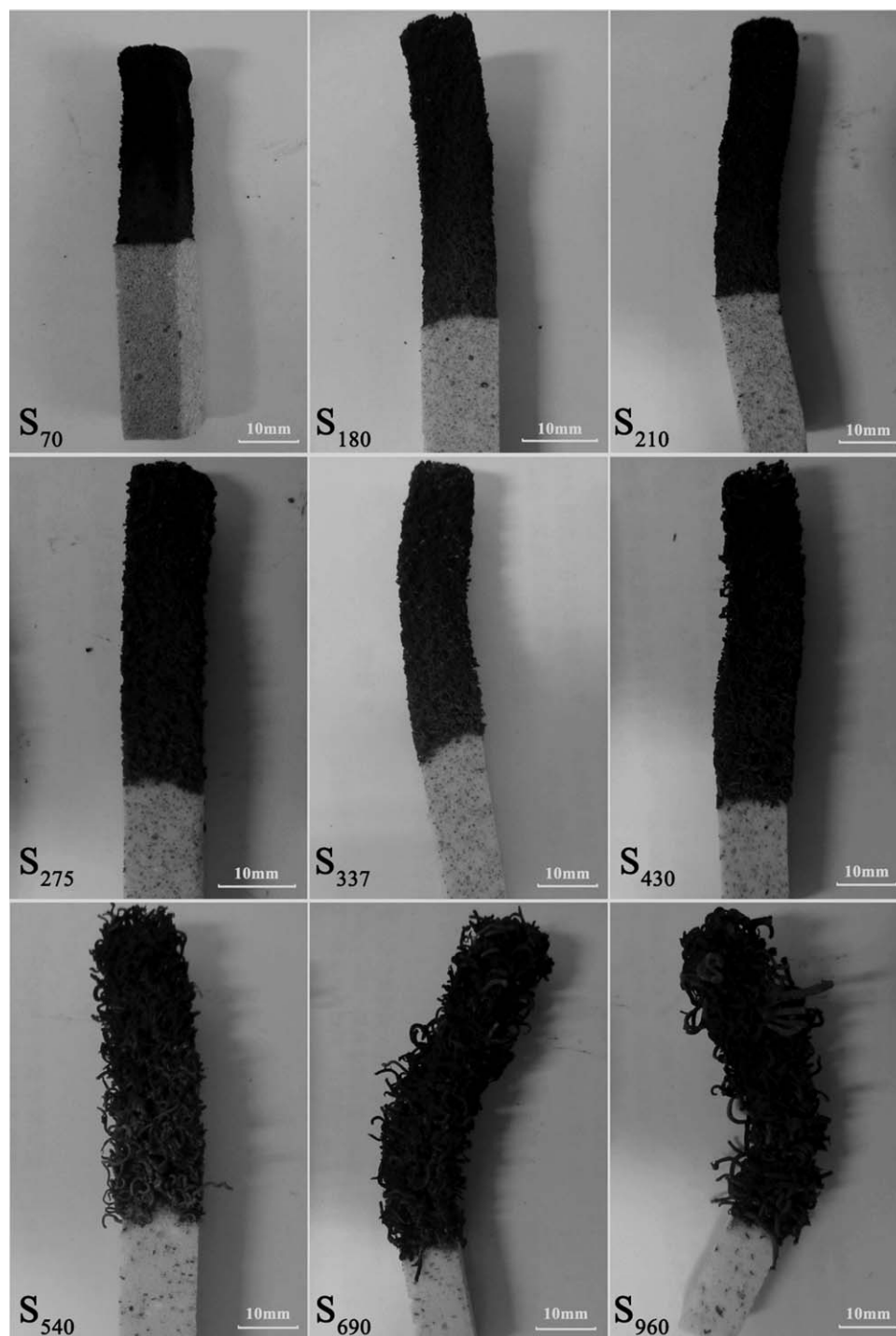
Figure 8. Digital photographs of EG/SPF composites after LOI test (20 pphp).

interpreted as the number of small EG particles in an average foam volume was more than the larger particle systems and the exfoliated graphite formed during the heat treatment process was not beneficial to the heat penetration which improving the thermal stability of SPF. The DTG thermograms show that the value of T_{max} had a slight decrease while in the presence of EG. In addition, in the case of PU/EG a shoulder peak was

observed between 260 and 320°C. This may be attributed to the oxidation and fragmentation process of the polymer matrix accelerated by the residual nitric acid in the EG interlayer.[25] Moreover, the nitric acid can react with graphite at high temperature[26]:

$$C + 4HNO_3 \xrightarrow{\text{High Temperature}} CO_2\uparrow + 2H_2O\uparrow + 4NO_2\uparrow$$
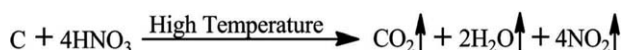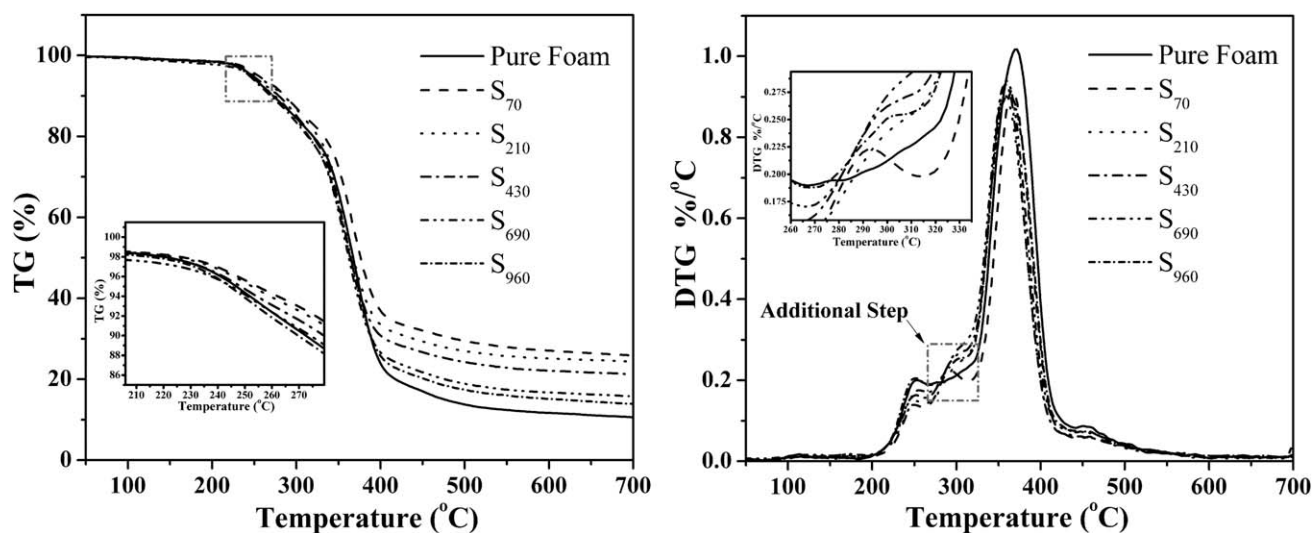
Figure 9. The TG and DTG curve of SPF with different EG additives (under nitrogen atmosphere).

In Table IV, composite systems exhibited higher residues than the neat foam at high temperature which was because of the higher thermal stability of the expanded graphite formed by the EG particles. It can also find from the table that composite filled with small size of EG have a higher residual weight than the bigger size of EG filled composite. This may be ascribed to the fact that bigger size of EG have higher expanded volume and more generated gases than that of small size which resulted in less residual char.

In brief, TGA analysis showed that the presence of EG particles and its size exhibited minor effects on the thermal stability of the SPF composites. SPF filled with small particle size of EG showed a higher residue than the other composite systems.

Mechanical Properties

As a kind of packaging material, the mechanical properties of SPFs are important parameters which of determining its application. It is known that the presence of filler has a tremendous effect on the mechanical properties of the polymer matrix. Compression studies were conducted to study the size effect of EG on the mechanical properties of SPFs. In Figure 10, the compressive strength at 25% strain of EG filling SPF is significantly higher than the neat foam. This was mainly due to the

presence of graphite, which could effectively limit the deformation of the foam samples. However, the compression strength and Young's modulus of SPFs is seen in concave pattern with the increase of EG particle size, while the minimum value appears at the EG particle size of 400 μm.

Graphite flakes can go across multiple cells with the increasing particle size of EG. In Figure 2(d), the interfacial adhesion between the graphite particles and the matrix was weak. When the sample was compressed, slippage might occur between the graphite and matrix, resulting in the decrease of strength and modulus of EG/SPF. Small size of EG distributed in the foam matrix [Figure 2(c)] and had a slight effect on the compressive properties. With the increase in the EG size, defects caused by the EG particles became larger and compressive properties of the composite decreased. On the other hand, the increase of EG size led to a decrease of the particle numbers. Although defects caused by the large particle size EG became obvious, the reduction in the number of defects made the strength of the foam rise again.

Table IV. Experimental Data of TGA Analysis

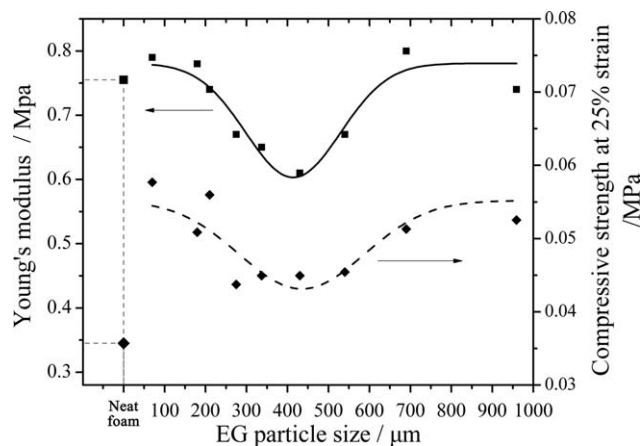| Material	$T_{5wt\ \%}$ (°C)	T_{max} (°C)	Residue in 700°C (%)
Pure SPF	247.0	369.8	10.56
S_{70}	254.6	366.5	25.86
S_{210}	252.5	357.8	24.40
S_{430}	248.5	357.5	21.18
S_{690}	245.2	360.2	15.80
S_{960}	244.7	362.7	13.88

Figure 10. The mechanical properties of SPF/EG composites.

CONCLUSIONS

Semi-rigid polyurethane foam based composites were produced by addition of different EG particle size and the effect on the flame retardant properties was studied. SPF with EG of smaller than about 150 μm, showed few improvement on fire-retardant performance of SPF compared to neat one. EG/SPF composites exhibited significant improvement in flame retardant properties after graphite size larger than about 150 μm. This improvement was significant for larger size EG, which was attributed to formation of a surface isolation layer during burning. Horizontal burning test also confirmed the conclusion. Attributed to the reduction in the number of EG particles, a turning point was observed at the particle size of 430 μm after which the LOI value improved slowly. TGA analysis showed that EG particles and its size exhibited minor effects on the thermal stability of the SPF composite. In the current investigation, SPFs filled with medium particle size (400 μm) of EG showed poor compression performance.

ACKNOWLEDGMENTS

REFERENCES

1. Mitsuru, S.; Atsushi, I.; Masayoshi, M. US Patent 6,306,918 Bl, **2001**.

2. Armistead, J. P.; Wilkes, G. L. *J. Appl. Polym. Sci.* **1988**, *35*, 601.

3. Mispreuve, H. L. S. A.; Waddington, S.; Tribelhorn U. US Patent 5,484,820, **1996**.

4. Wang, J. Q.; Chow, W. K. *J. Appl. Polym. Sci.* **2005**, *97*, 366.

5. Dresselhaus, M. S.; Dresselhaus, G. *Adv. Phys.* **1981**, *30*, 139.

6. Li, J.; Feng, L.; Jia, Z. *Mater. Lett.* **2006**, *60*, 746.

7. Modesti, M.; Lorenzetti, A. *Polym. Degrad. Stab.* **2002**, *78*, 167.

8. Modesti, M.; Lorenzetti, A. *Eur. Polym. J.* **2003**, *39*, 263.

9. Zhang, X.-G.; Ge, L. L.; Zhang, W. Q.; Tang, J. H.; Ye, L.; Li, Z. M. *J. Appl. Polym. Sci.* **2011**, *122*, 932.

10. Modesti, M.; Lorenzetti, A.; Simioni, F.; Camino, G. *Polym. Degrad. Stab.* **2002**, *77*, 195.

11. Wolska, A.; Goździkiewicz, M.; Ryszkowska, J. *J. Mater. Sci.* **2012**, *47*, 5627.

12. Wolska, A.; Goździkiewicz, M.; Ryszkowska, J. *J. Mater. Sci.* **2012**, *47*, 5693.

13. Duquesne, S.; Delobel, R.; Bras, M. L.; Camino, G. *Polym. Degrad. Stab.* **2002**, *77*, 333.

14. Shi, L.; Li, Z. M.; Yang, M. B.; Yin, B.; Zhou, Q. M.; Tian, C. R.; Wang, J. *Polym. Plast. Technol. Eng.* **2005**, *44*, 1323.

15. Thirumal, M.; Khastgir, D.; Singha, N. K.; Manjunath, B. S.; Naik, Y. P. *J. Appl. Polym. Sci.* **2008**, *110*, 2586.

16. Gharehbaghi A.; Bashirzadeh R.; Ahmadi Z. *J. Cell Plast.* **2011**, *47*, 549.

17. Xie, R.; Qu, B. *J. Appl. Polym. Sci.* **2001**, *80*, 1181.

18. Li, Z. Z.; Qu, B. *J. Polym. Degrad. Stab.* **2003**, *81*, 401.

19. Kuan, C. F.; Yen, W. H.; Chen, C. H.; Yuen S. M.; Kuan H. C.; Chiang C. L. *Polym. Degrad. Stab.* **2008**, *93*, 1357.

20. Zaikov, G. E.; Lomakin, S. M. *J. Appl. Polym. Sci.* **2002**, *86*, 2449.

21. Shi, L.; Xie, B. H.; Wang, J.-H.; Tian, C. R.; Yang, M. B. *Polym. Int.* **2006**, *55*, 862.

22. Bian, X. C.; Tang, J. H.; Li, Z. M.; Lu, Z. Y.; Lu, A. *J. Appl. Polym. Sci.* **2007**, *104*, 3347.

23. Chattopadhyay D. K., Webster D. C. *Prog. Polym. Sci.* **2009**, *34*, 1068.

24. Chuang F. S. *Polym. Degrad. Stabil.* **2007**, *92*, 1393.

25. Duquesne, S.; Bras, M. L.; Bourbigot, S.; Delobel, R.; Camino, G.; Eling, B.; Lindsay, C.; Roels, T. *Polym. Degrad. Stab.* **2001**, *74*, 493.

26. Wang, B. B.; Hu S.; Zhao K. M.; Lu H. D.; Song L.; Hu Y. *Ind. Eng. Chem. Res.* **2011**, *50*, 11476.